BJP British Journal of Pharmacology

DOI:10.1111/bph.13083
www.brjpharmacol.org

RESEARCH PAPER

In vitro and *in vivo* regulation of synaptogenesis by the novel antidepressant spadin

C Devader, A Khayachi, J Veyssière, H Moha ou Maati*, M Roulot, S Moreno, M Borsotto, S Martin, C Heurteaux and J Mazella

CNRS, Institut de Pharmacologie Moléculaire et Cellulaire, UMR 7275, Université de Nice-Sophia Antipolis, Valbonne, France

Correspondence
Jean Mazella, Institut de Pharmacologie Moléculaire et Cellulaire, UMR 7275, Université de Nice-Sophia Antipolis, 660 route des Lucioles, 06560 Valbonne, France. E-mail: mazella@ipmc.cnrs.fr

*Present address: Institut de Génomique Fonctionnelle, UMR 5203 CNRS/INSERM/UM1/UM2, 141 rue de la Cardonille, 34095 Montpellier Cedex 5, France.

Received
24 June 2014
Revised
10 December 2014
Accepted
8 January 2015

BACKGROUND AND PURPOSE

We have described a novel antidepressant peptide, spadin, that acts by blocking the TWIK-related-potassium channel, type 1 (TREK-1). Here, we examined possible mechanisms of action of spadin at both molecular and cellular levels.

EXPERIMENTAL APPROACHES

Effects of spadin were measured in primary cultures of neurons or tissues from mice injected i.v. with spadin. Western blots, qPCR, histochemical and electrophysiological techniques were used.

KEY RESULTS

In vitro, spadin increased neuronal membrane potential and activated both the MAPK and PI3K signalling pathways, in a time- and concentration-dependent manner. The latter pathway was involved in the protective effect of spadin against staurosporine-induced apoptosis. Also, spadin enhanced both mRNA expression and protein of two markers of synaptogenesis, the post-synaptic density protein of 95 kDalton (PSD-95) and synapsin. We confirmed these effects on synaptogenesis by the observation that spadin treatment significantly increased the proportion of mature spines in cortical neurons. Finally, *in vivo* injections of spadin led to a rapid increase in both mRNA expression and protein level of brain-derived neurotrophic factor (BDNF) in the hippocampus, confirming the antidepressant action of the peptide. We argue for a new role of spadin in synaptogenesis as both PSD-95 and synapsin mRNA expression and protein levels were further enhanced in the hippocampus, following treatment *in vivo* with the peptide.

CONCLUSIONS AND IMPLICATIONS

These findings provide new mechanisms of action for the rapidly acting antidepressant peptide spadin by stimulating expression of BDNF and synaptic proteins, both *in vitro* and *in vivo*.

Abbreviations

BDNF, brain-derived neurotrophic factor; LY294002, 2-morpholin-4-yl-8-phenylchromen-4-one; mTOR, mammalian target of rapamycin; NTSR3, neurotensin receptor-3; PD98059, 2′-amino-3′-methoxyflavone; PSD-95, post-synaptic density protein of 95 kDalton; TREK-1, TWIK-related-potassium channel, type 1

Tables of Links

TARGETS
Ion channel[a]
TREK-1,. K_{2P}2.1 channel
Enzymes[b]
Akt
Caspase-3
ERK1/2
mTOR
PI3K

LIGANDS
BDNF
Fluoxetine
Ketamine
LY294002
PD98059
Staurosporine

These Tables list key protein targets and ligands in this article which are hyperlinked to corresponding entries in http://www.guidetopharmacology.org, the common portal for data from the IUPHAR/BPS Guide to PHARMACOLOGY (Pawson *et al.*, 2014) and are permanently archived in the Concise Guide to PHARMACOLOGY 2013/14 ([a,b]Alexander *et al.*, 2013a,b).

Introduction

The origins and causes of depression are diverse, and therefore do not facilitate the diagnosis of the pathology. Molecules developed to treat depression include the tricyclic antidepressants, inhibitors of MAO-A or 5-HT selective reuptake inhibitors (see Berton and Nestler, 2006). Nevertheless, many other atypical antidepressant drugs were also developed such as mianserine, tradozone (Boschmans *et al.*, 1987; Fagiolini *et al.*, 2012), mirtazapine (Dolder *et al.*, 2012), agomelatine (Srinivasan *et al.*, 2012), tianeptine (McEwen and Olie, 2005), scopolamine (Drevets *et al.*, 2013), ketamine or lanicemine (Zarate *et al.*, 2006; Sanacora *et al.*, 2014).

The antidepressant drugs do not provide a fully satisfactory treatment, for several important reasons: (i) one-third of patients are resistant to the drugs (Pacher and Kecskemeti, 2004); (ii) there is a delayed onset of antidepressant drug action (Fava and Kendler, 2000; Nestler *et al.*, 2002); and (iii) antidepressant drug treatments have numerous deleterious side effects (Sicouri and Antzelevitch, 2008; Thase and Denko, 2008).

Taking into account the mental health of millions of people worldwide and the associated economic burden, it is now crucial to develop alternative strategies aimed at developing novel antidepressants that could potentially show higher rates of efficacy and lower rates of side effects. We previously reported that an endogenous peptide of 44 amino acids (PE) released from the maturation of the neurotensin receptor-3 (NTSR3) (Mazella *et al.*, 1998; Munck Petersen *et al.*, 1999), also called sortilin (Petersen *et al.*, 1997), displays potent antidepressant effects in several tests performed in mice (Mazella *et al.*, 2010). We isolated an active sequence of 17 amino acids from this peptide, named spadin, which exerts its antidepressant properties through the blockade of the TWIK-related-potassium channel, type 1 (TREK-1) (K_{2P}2.1; Mazella *et al.*, 2010). TREK-1 channels are activated by stretch, polyunsaturated fatty acids, warm temperatures, internal acidosis and volatile anaesthetics (Honore, 2007). They are inhibited by fluoxetine and blocked by phosphorylation processes. Deletion of the TREK-1 gene (*kcnk2*) leads to mice that display a depression-resistant phenotype, which mimics treatment with antidepressants (Heurteaux *et al.*, 2006b). Spadin binds to TREK-1 with an affinity of 10 nM, blocks its activity and induces its sequestration into cells. The interaction of spadin with TREK-1 does not show any striking side effects and does not interfere with any known TREK-1-controlled functions (Moha Ou Maati *et al.*, 2012). *In vivo*, spadin increases the firing rate of serotonergic neurons from the dorsal raphe nucleus and activates hippocampal neurogenesis (Mazella *et al.*, 2010). Moreover, NTSR3/sortilin directly interacts with TREK-1 to regulate its plasma membrane localization (Mazella *et al.*, 2010). Both proteins are colocalized in neurons within the dorsal raphe nucleus and have been previously shown to be expressed in several brain areas known to be involved in depression including the prefrontal cortex, amygdala, hippocampus, nucleus accumbens, dorsal raphe and hypothalamus (Hervieu *et al.*, 2001; Sarret *et al.*, 2003).

Spadin exhibits antidepressant properties, when injected in mice (Mazella *et al.*, 2010), and induced a rapid hippocampal neurogenesis after a 4 day treatment. However, its cellular mechanisms of action as well as the demonstration that new neurons are functional have not yet been characterized. Moreover, the rapid onset of action of spadin, which can be compared with the rapidly acting antidepressant ketamine (Li *et al.*, 2011; Dwyer and Duman, 2013), prompted us to evaluate the effect of spadin on the induction of synaptogenesis and spine maturation. The mechanisms of action of spadin were determined in primary cultures of neurons from embryonic and post-natal mice. We performed electrophysiological and biochemical experiments to study the membrane function and the intracellular signalling of the peptide followed by qPCR and Western blot analyses of proteins involved in synaptogenesis and whose expression is altered in mood disorders such as post-synaptic density protein of 95 kDalton (PSD-95), synapsin and brain-derived neurotrophic factor (BDNF). Neuronal spine maturation has been visualized using confocal imaging of GFP-transfected neurons. We confirmed the effects we observed *in vitro*, on synaptic proteins by *in vivo* injection of spadin followed by protein analysis in samples of hippocampus and prefrontal cortex.

Methods

Animals

All animal care and experimental procedures complied with the policies on the care and use of laboratory animals of European Community legislation 2010/63/EU and were approved by the local Ethics Committee (CIEPAL) (protocol number 00893.02). All studies involving animals are reported in accordance with the ARRIVE guidelines for reporting experiments involving animals (Kilkenny *et al.*, 2010; McGrath *et al.*, 2010). A total of 100 animals were used in the experiments described here. We used C57Bl/6J male mice (20–25 g) from Janvier Labs (St Berthevin, France).

Primary neuronal cultures

Mice were anaesthetized by inhalation of 2% isoflurane mixed with 30% oxygen and 70% nitrous oxide and then killed. Embryos (E14) were removed and brain cortices dissected in PBS containing 1% glucose. Neurons were also prepared from cerebral cortices of 3-day-old mice, as described by Brewer and Torricelli (2007). Dissociated neurons were plated on poly-L-lysine-treated dishes and cultured up to 18 days in neurobasal medium containing 2% B27 and 50 $\mu g \cdot mL^{-1}$ gentamycin at 37°C under 5% CO2.

Spadin iodination

Spadin (2 nmol) was iodinated with [^{125}I]NaI (0.5 nmol) using lactoperoxidase as oxidant. Monoiodinated spadin (on Tyr-0) was purified by HPLC using a Waters apparatus equipped with a RP18 Lichrosorb column (Macherey-Nagel, Düren, Germany). Elution was carried out at a flow rate of 1 $mL \cdot min^{-1}$ with a linear gradient of increasing concentration from 30 to 60% of acetonitrile in water containing 0.1% TFA in 36 min. The iodinated peptide was eluted at 24 min.

Binding assays

Cultures of cortical neurons were incubated with 0.4 nM [^{125}I]-spadin (400 000 cpm in 250 µL). Incubations were performed in Earle's-Tris-HEPES buffer pH 7.4, containing 140 mM NaCl, 5 mM KCl, 1.8 mM $CaCl_2$, 3.6 mM $MgCl_2$ and 0.1% BSA in the presence of increasing concentrations of non-radioactive spadin (from 10^{-10} to 10^{-5}M). Incubations were terminated by washing cells twice with 2 mL of Earle's-Tris-HEPES buffer. The radioactivity bound to neurons was recovered with 1 M NaOH (1 mL) and counted with a gamma-counter.

Electrophysiological experiments

Whole cell current recordings were performed on primary cortical mouse neurons seeded at a density of 1 200 000 cells per 35 mm dish 10 days before testing. Membrane potentials were measured on cortical neurons after 1 h of incubation in control conditions (water for the vehicle), in the presence of 1 µM of spadin. Cells were then patched and membrane potentials immediately measured using the whole-cell, patch-clamp configuration. All membrane potentials values are expressed in mV as mean ± SEM. IV curves were realized for each cell in control conditions and in the presence of 1 µM of spadin. Global current was recorded using the whole-cell configuration of the patch-clamp technique. Each current was calculated using an RK 400 patch-clamp amplifier (Axon Instrument, Sunnyvale, CA, USA), low-pass filtered at 3 kHz and digitized at 10 kHz using a 12-bit analogue-to-digital converter digidata (1322 series, Axon Instrument). The bath solution contained (in mM) 150 NaCl, 5 KCl, 3 $MgCl_2$, 1 $CaCl_2$ and 10 HEPES adjusted to pH 7.4 with NaOH. The pipette solution contained (in mM) 155 KCl, 3 $MgCl_2$, 5 EGTA and 10 HEPES adjusted to pH 7.2 with KOH. Stimulation protocols and data acquisition were carried out at room temperature using a microcomputer (Dell Pentium, Montpellier, France) and the pClamp 8.2 commercial software (Molecular Devices, Wokingham, UK). Cells were clamped at –80 mV and voltage changes applied by step of 20 mV (from –100 to +60 mV). Duration of depolarization pulses was 0.825 ms and the pulse cycling rate was 5 s. Current amplitudes were calculated at the end of stimulation pulses. Current amplitudes were expressed in current densities.

Western blotting

Mouse cortical neurons treated with the indicated effectors for various times were homogenized in Laemmli buffer and analysed using 10% SDS PAGE gels. Separated proteins were then transferred from gels onto nitrocellulose membranes (VWR, Fontenay-sous-Bois, France) and blocked either with 5% skim milk or 5% BSA as indicated in PBS for 30 min at room temperature. Membranes were incubated with antibodies directed against PSD-95, synapsin or BDNF overnight at 4°C. Tubulin contents were determined after stripping using a 1/1000 dilution anti-tubulin antibodies (Sigma-Aldrich, Saint-Quentin Fallavier, France). After four washes in 0.1% Tween/PBS, secondary anti-mouse or anti-rabbit HRP-conjugated antibodies (Amersham Biosciences, Orsay, France; 1/10000) were incubated for 1 h at room temperature. Proteins were detected with the ECL plus detection reagents (Amersham Biosciences) using an LAS-3000 imaging system (Fujifilm, Düsseldorf, Germany). Relative intensities of the labelled bands were analysed by densitometric scanning using ImageJ software (Wayne Rasband, National Institute of Health, Bethesda, MD, USA). Protein activation was normalized using total tubulin as indicated.

Caspase-3 activity measurements

Neurons were plated in 12-well dishes for 10–14 days before experiments. Neurons were incubated for 2–4 h with 1 µM staurosporine (Sigma-Aldrich) in the absence or in the presence of 1 µM spadin. Caspase-3 activity was measured using Ac-DEVD-7-AMC (Sigma-Aldrich) as a substrate (Coppola *et al.*, 2008).

Primer design and real-time qPCR

Primers (Eurogentec, Angers, France), designed as previously described (Dingemans *et al.*, 2010), were specific for sequences of PSD-95, synapsin, BDNF and GAPDH and CycloD as reference genes (Table 1). Real-time qPCR was performed on the LightCycler™ 480 (Roche, Meylan, France) using the LightCycler™ 480 SYBR Green 1 Master mix (Roche). PCR reactions were performed in 20 µL volume containing 16 ng cDNA, 10 µL 2× LightCycler™ 480 SYBR Green 1 Master mix and 1 µL of primer mix (10 µM forward primer, 10 µM reverse primer).

Table 1
Primers used in qPCR experiments

	Forward	Reverse
PSD-95	5′-CGCTACCAAGATGAAGACACG-3′	5′-CAATCACAGGGGGAGAATTG-3′
Synapsin	5′-GGAAGGGATCACATTATTGAGG-3′	5′-TGCTTGTCTTCATCCTGGTG-3′
BDNF	5′-AGTCTCCAGGACAGCAAAGC_3′	5′-TGCAACCGAAGTATGAAATAACC_3′
Gapdh	5′-GAACATCATCCCTGCATCC-3′	5′-CCAGTGAGCTTCCCGTTCA-3′
CycloD	5′-AAGGATGGCAAGGATTGAAA-3′	5′-GCAATTCTGCCTGGATAGCTT-3′

The PCR profile was as follows: 5 min at 95°C, followed by 45 cycles of 10 s at 95°C, 10 s at 60°C and 10 s at 72°C.

The Ct value of each gene of interest was normalized to the Ct of the reference genes: $\Delta Ct = Ct_{goi} - Ct_{ref}$ with $Ct_{ref} = (Ct_{GAPDH} \times Ct_{CycloD})^{(1/2)}$ with $_{goi}$ = gene of interest, and $_{ref}$ = reference gene. $\Delta\Delta CT$ = ΔCT experimental condition – ΔCT control condition. Values were expressed as $2^{-\Delta\Delta Ct}$ normalized using saline solution-injected animals as control. For experiments performed from newborn cerebral cortex values are expressed as $2^{-\Delta Ct}$.

Analysis of spine morphology

Primary cortical neurons were treated every day for 18 days with spadin (2 μL; final concentrations 10 nM or 1 μM). Half of the medium was changed every 3 days. Neurons were then transduced with attenuated Sindbis virus (Martin *et al.*, 2008) expressing GFP for 22 h before use. For imaging experiments, neurons were fixed at 19 days *in vitro* in PBS containing 3.7% formaldehyde and 5% sucrose for 1 h at room temperature. Fixed neurons were then rinsed twice with PBS at room temperature and mounted in Mowiol (Sigma) before confocal examination.

Sequential confocal images (1024 × 1024 pixels) were acquired with a 63× oil-immersion lens with Numerical Aperture, 1.4 on an inverted TCS-SP5 confocal microscope (Leica Microsystems, Nanterre, France). Z-series of six to eight images of randomly selected GFP-expressing dendrites were compressed into two dimensions using the maximum projection algorithm of the Leica software. We analysed ~3500 spines per condition from secondary dendrites (~3 dendrites per neuron, 20 neurons per condition). At the time of acquisition, laser power was adjusted so that all spines were below the threshold of saturation. To analyse dendritic protrusions, projection images were imported into Neuronstudio software (Rodriguez *et al.*, 2008), which allows for the automated detection of dendrites, immature and mature spines. The length of individual spines was automatically measured and data were imported in GraphPad Prism software for statistical analysis.

In vivo *injection of spadin*

Prior to injection, 8- to 12-week-old male C57BL/6J were warmed for 5–10 min with an overhead heat lamp to dilate the veins. Then, they were placed in a constrained box and injected in the caudal vein with 100 μL of either 1 μM spadin or 0.9% NaCl solution. For mRNA expression and protein content of PSD-95 and synapsin, mice were injected once a day for 4 days, then groups of mice (six per group) were killed on days 7, 14 and 21, after the first day of injection. The brain was removed and the indicated cerebral regions were dissected and analysed by qPCR or Western blotting, as described earlier.

Data analysis

Results are presented as means ± SEM from four to six determinations. However, statistical significance was calculated from median values obtained using the non-parametric Kruskal–Wallis test. For spine morphogenesis experiments, values represent means ± SEM. All experiments were repeated at least three times. Statistical significance for group comparisons was analysed by ANOVA with a Newman–Keuls post-test. Normality for all groups was verified using the Shapiro-Wilk test. According to the Levene variance test, variances were homogenous for the percentage of mature spines and for the length of immature spines ($F = 0.25$; $P = 0.77$ and $F = 0.42$; $P = 0.65$ respectively). Cumulative plot data were analysed by the Kolmogorov–Smirnov test (K–S test). $P < 0.05$ was considered significant.

Materials

The peptide, spadin, with the following amino acid sequence: Y-APLPRWSGPIGVSWGLR (GenBank NM_019972 for mouse) was synthetized by Genecust (Dudelange, Luxemburg). Neurobasal medium and complementary medium B27 were from Invitrogen (Fisher Scientific, Illkirch, France). Gentamycin, 1–10-phenanthroline, Bovine Serum Albumin (BSA), fluoxetine, mammalian protease and phosphatase inhibitor cocktails were from Sigma France. Antibodies against the phosphorylated or total forms of ERK 1/2 and Akt were from Santa Cruz Laboratory, Inc. (Heidelberg, Germany). The antibodies against phospho-Akt, PSD-95, phospho-mammalian target of rapamycin (mTOR), BDNF and synapsin were from Cell Signaling (Ozyme, Montigny-le-Bretonneux, France).

Results

Spadin binding to neurons leads to neuronal depolarization

To characterize the cellular effects of the antidepressant spadin on mouse cortical neurons, we first performed direct binding experiments using a radiolabelled spadin peptide on living cells (Figure 1A). Competition experiments between [^{125}I]-spadin and unlabelled spadin indicated that spadin bound specifically to cortical neurons. The displacement curve

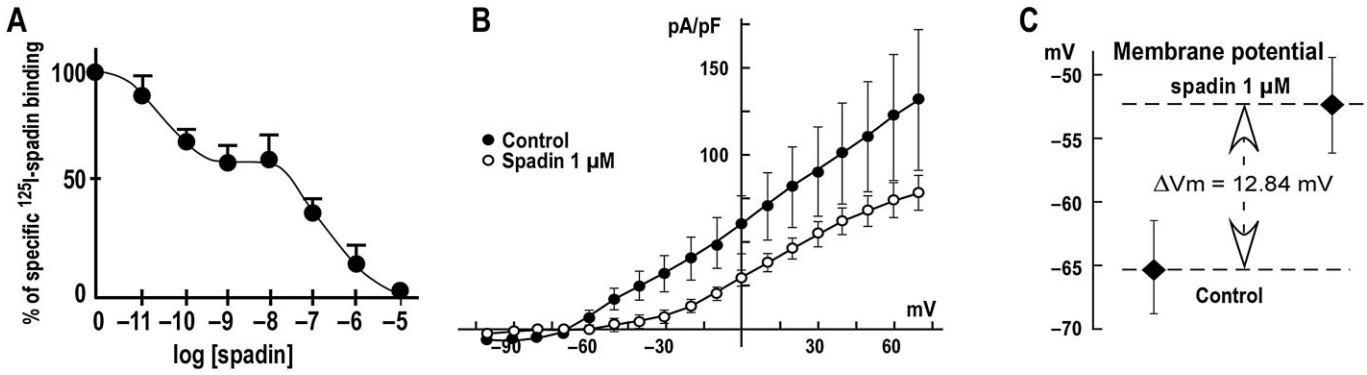

Figure 1

Spadin binding to neurons in culture triggers neuronal depolarization and drives endocytosis. (A) Competition between ^{125}I-spadin and unlabelled spadin for binding to mouse cortical neurons. Each point represents the mean ± SEM of duplicate determinations from three independent experiments. (B and C) I-V curves and membrane potentials on primary cortical embryonic mouse neurons recorded after 1 h incubation in control conditions (vehicle) and in the presence of spadin 1 µM. (B) I-V curves obtained in control conditions and in the presence of spadin 1 µM. (C) membrane potential mean values obtained in the two different conditions.

revealed the existence of two binding sites with corresponding IC_{50} values of 0.05 nM for the binding component representing 40% of the total binding, and of 100 nM for the 60% remaining binding (Figure 1A). Electrophysiological recordings on whole cells confirmed that the binding of spadin to neurons was functional. Indeed, I-V curves (Figure 1B) and membrane potentials (Figure 1C) recorded on cortical neurons 1 h after spadin (1 µM) incubation indicated that the peptide efficiently depolarized neurons, as expected from a blocking action on TREK-1 channels. Consequently, spadin induced an increase in the membrane potential with a ΔVm of 12.84 mV ± 2.28 (Figure 1C). We also confirmed that spadin dynamically regulates the membrane levels of both TREK-1 and sortilin in cortical neurons (Supporting Information Fig. S1).

To perform signalling and protein expression experiments *in vitro* and *in vivo*, we first needed to know the half-life time of the peptide when exposed to neuronal cultures, and second, its ability to cross the blood–brain barrier and to reach the brain following i.v. injection. The stability of spadin was measured on reverse-phase HPLC after incubation for various times with the cultured neuronal medium or mouse serum (Supporting Information Fig. S2). After 60 min of incubation on neurons, about half of the initial spadin remained intact whereas almost all the peptide was degraded after 60 min in mouse serum indicating that spadin is more stable at the vicinity of neurons than in serum. These results allowed us to determine how frequently spadin should be added to the primary neurons to maintain its activity.

To differentiate spadin recovered in the brain after i.v. injection, from other endogenous peptides present in the brain, we incorporated a fluorophore on the peptide (Atto 488 from Atto-Tec GmbH, Siegen, Germany) exhibiting a high e_{max} at 500 nm (9×10^4 $M^{-1} \cdot cm^{-1}$). This allowed us to determine, using HPLC, that about 1% of the labelled peptide was recovered in the brain in its intact form 30 min after i.v. injection (Supporting Information Fig. S2). This observation is in line with our initial finding that peripheral administration of spadin can induce central antidepressant effects (Mazella *et al.*, 2010).

Functional signalling of spadin in cortical neurons

We investigated the intracellular signalling pathways activated by spadin in cultured neurons from embryos. Spadin (100 nM) rapidly stimulated the phosphorylation of ERK1/2 and Akt, but not of mTOR (Figure 2A) whereas ketamine, used as a positive control, induced phosphorylation of mTOR (Figure 2A). The latter observation is in agreement with the mTOR-dependent antidepressant effects of ketamine (Li *et al.*, 2010). We confirmed that spadin was able to activate the same signalling pathways (i.e. ERK1/2 and Akt) in neurons prepared from new-born mice (Figure 2B). Standardization of signalling pathways using antibodies against non-phosphorylated proteins indicated a twofold stimulation from 15 to 60 min for phospho-ERK1/2 (Figure 2C), a two- to threefold stimulation up to 60 min for phospho-Akt (Figure 2D), and an absence of spadin effect on phospho-mTOR (Figure 2E). ERK phosphorylation was maximum for 100 nM spadin (Figure 2F). We confirmed that ERK1/2 activation in response to spadin was blocked in the presence of the MAPK inhibitor PD98059 (Figure 2F). Similarly to ERK phosphorylation, the concentration of spadin that maximally increased Akt phosphorylation was 100 nM (Figure 2G). As expected, when neurons were pretreated with the PI3K inhibitor LY294002, the phosphorylation of Akt in spadin-treated neurons was abolished (Figure 2G).

As the PI3K pathway is involved in cell survival, we investigated the effect of spadin on protection against staurosporine-induced caspase-3 activation in neuronal cultures. We found that a 4 h incubation of cortical neurons with 1 µM staurosporine significantly increased caspase-3 activity (Figure 2H) and spadin inhibited 70% of the staurosporine-induced caspase-3 activation (Figure 2I). This effect was dependent on PI3K, as LY294002, a specific inhibitor of this pathway, reversed the protective effect of spadin but the MAPK inhibitor PD98059 was not effective (Figure 2I). These results therefore demonstrated that spadin

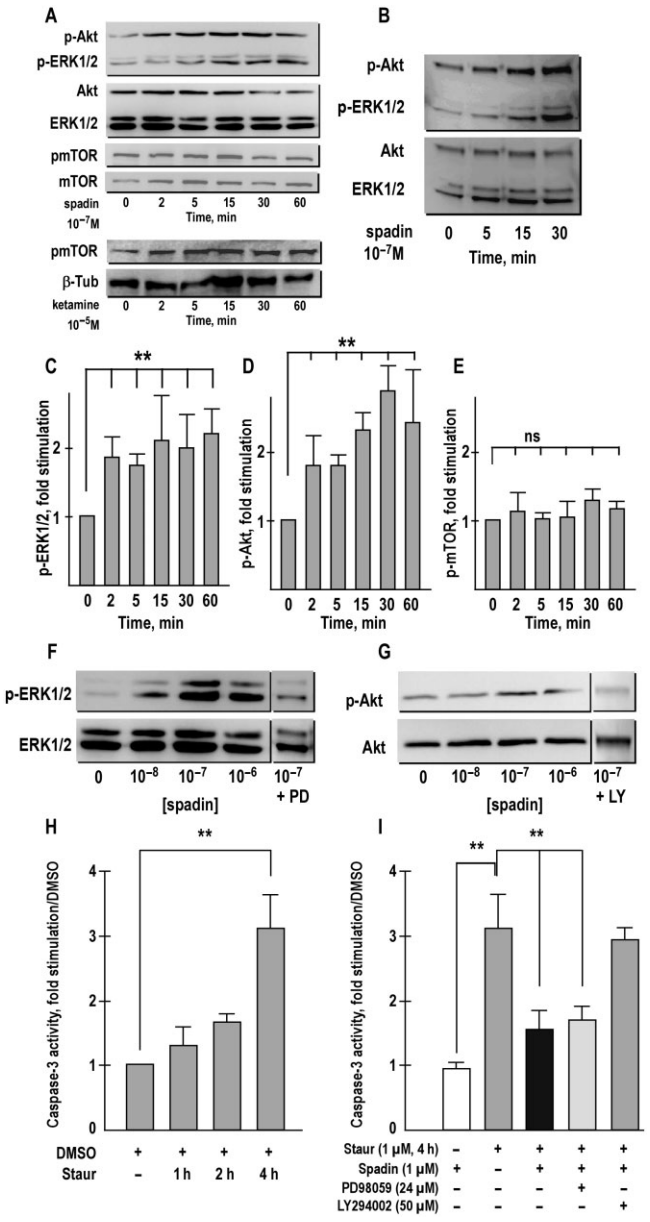

Figure 2

Effect of spadin on ERK1/2 and Akt phosphorylation in cortical neurons. (A) Neurons prepared from 14-day-old embryos were incubated with 10^{-7}M spadin or 10 μM ketamine (1 μL of a 1000× solution) for various times at 37°C. The phosphorylation of ERK, Akt and mTOR was determined by immunoblotting using antibodies directed against the phosphorylated active forms of both kinases. (B) Neurons prepared from 3-day-old mice were stimulated with 10^{-7}M spadin for indicated times at 37°C. The phosphorylation of Erk, Akt was determined by immunoblotting using antibodies directed against the phosphorylated active forms of both kinases. (C–E) Data were standardized from three to five different experiments using the labelling obtained on the same blot with antibodies directed against the total forms of ERK1/2, Akt and mTOR and expressed as means ± SEM. $^{**}P < 0.05$, significantly different as indicated. ns, non-significant. (F and G) Neurons were incubated with various concentrations of spadin for 15 min at 37°C. Phosphorylation of ERK1/2 (F) and Akt (G) was determined as described in A. PD98059 and LY294002 are specific inhibitors of ERK and Akt kinases respectively. (H) Effect of staurosporine on caspase-3 activity in cortical neurons. Neurons were incubated for the indicated times with 1 μM staurosporine. Samples were processed for capsase-3 activity as described. Data are means ± SEM from three independent experiments and are expressed in arbitrary units. $^{**}P < 0.05$, significantly different as indicated. (I) Effect of spadin on staurosporine-induced caspase-3 activity. Neurons were treated for 4 h with 1 μM staurosporine in the absence or in the presence of 1 μM spadin with or without 24 μM PD98059 or 50 μM LY294002. Caspase-3 activity was measured as earlier. Data are means ± SEM from three experiments. $^{**}P < 0.05$, significantly different as indicated.

was a potent protector of neurons against cytotoxicity, through the activation of the PKB/Akt signalling pathway.

Spadin increases content of synaptic marker proteins and promotes the maturation of dendritic spines

We previously determined that a subchronic treatment with spadin in mice resulted in a rapid (4 days) activation of neurogenesis in the dentate gyrus through the phosphorylation of the transcription factor CREB (Mazella *et al.*, 2010), a factor known to be involved in neurogenesis (Carlezon *et al.*, 2005; Krishnan and Nestler, 2008). As synaptic alterations have been observed in depression and could therefore be a potential target for therapeutic intervention (Duman and Aghajanian, 2012), we explored the role of spadin on synaptogenesis. We first measured the effect of spadin on mRNA expression levels and protein content of two protein markers of synaptogenesis, PSD-95 and synapsin. Spadin transiently increased the mRNA expression levels of both PSD-95 and synapsin with a maximum expression observed 8 h after exposure to spadin (Figure 3A and B). We also analysed the mRNA expression of BDNF whose levels are known to be down-regulated during depression and up-regulated by antidepressants (Airan *et al.*, 2007). We observed a weak and transient increase of its mRNA expression, 5 h after spadin incubation (Figure 3C). At the protein levels, PSD-95 immunoreactivity was significantly increased 5 h post-treatment while the increase in synapsin protein occurred 36 h post-spadin treatment (Figure 3D and E). Despite the slight increase in BDNF mRNA expression levels, we were not able to detect any significant increase in the corresponding protein level (Figure 3F).

Synaptic dysfunction is generally correlated with deleterious alterations of spine morphology, which play crucial roles in major depressive disorders (Shansky *et al.*, 2009; Lin and Koleske, 2010; Duman and Aghajanian, 2012). Some antidepressant drugs are able to restore the density of dendritic spines (Norrholm and Ouimet, 2001). The various shapes of spines (thin, filopodia and mushroom) are associated with different stages of dendritic maturation, consequent on functional neuronal circuits (McKinney, 2010). Therefore, we tested the effect of spadin on the frequency and the morphology of dendritic spines in cultured neurons. We treated neurons *in vitro* for 18 days instead of only 4 days during the last 4 days of neuronal differentiation, in order to ensure assessments of the effects of spadin, over the whole

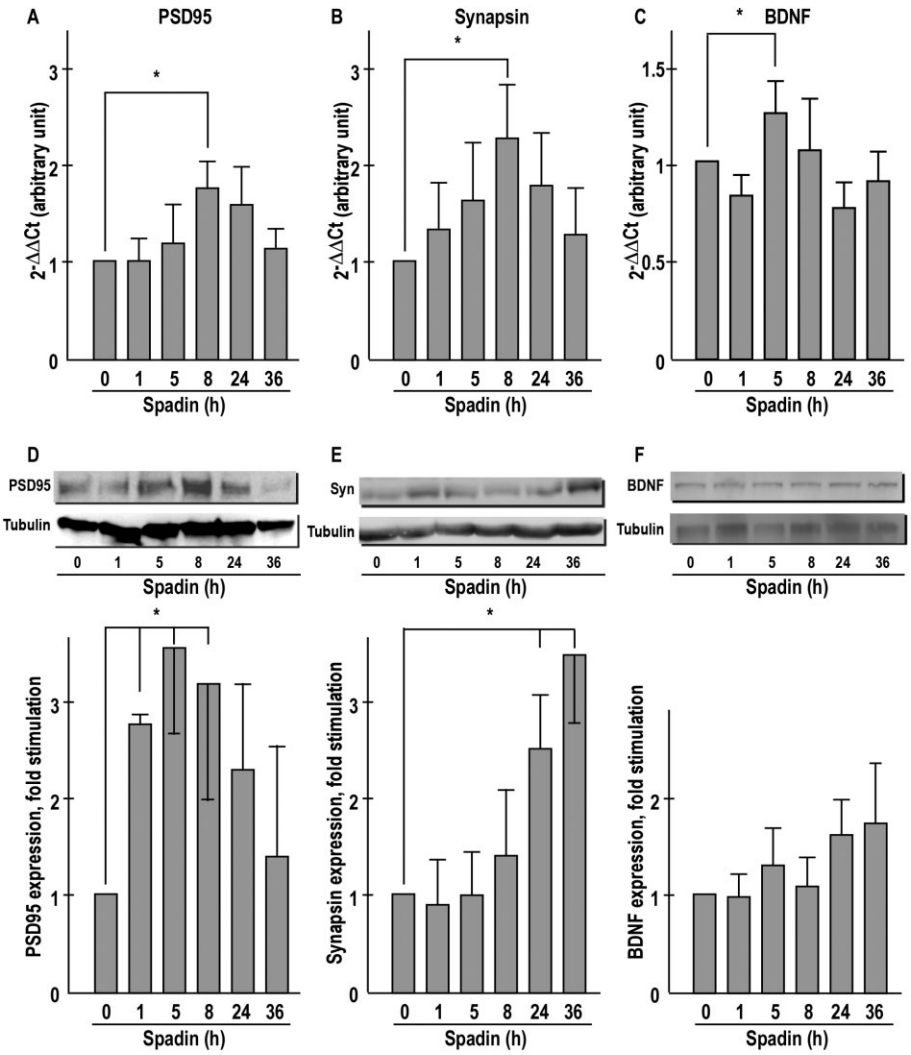

Figure 3

Spadin increases the expression of synaptic proteins in cortical neurons. (A–C) Neurons were incubated with 10^{-7}M spadin for the indicated times at 37°C. RNAs extracted from neurons were subjected to quantitative PCR. Bar graphs showing the mRNA expression of PSD-95 (A), synapsin (B) and BDNF (C) were normalized with the control condition (0). Histograms are mean ± SEM from three independent determinations, *$P < 0.05$, significantly different as indicated. (D–F) Neurons were incubated with 10^{-7}M spadin for indicated times at 37°C. The amount of PSD-95, synapsin and BDNF was determined by immunoblotting and using the labelling of the same blot with antibodies against β-tubulin. Immunoblots shown are representative of a typical experiment. The representation of the amount of each protein was expressed as fold increase compared with control conditions. Data are means ± SEM from three independent experiments. *$P < 0.05$, significantly different as indicated.

maturation period of neurons and not only the last 4 days, when neurons are already matured. Moreover, this longer treatment showed the lack of toxicity of the peptide when compared with identical treatment with either ketamine (10 μM) or fluoxetine (1 μM), which induced cell death after 1 week application (J. Mazella, unpubl. obs.). Figure 4A and B show dendrites from GFP-expressing neurons treated for 18 days with vehicle (PBS) or with 10 nM or 1 μM spadin. Spadin, at either concentration, did not affect the number of protrusions (Figure 4C), with the same protrusion frequencies of about 5 spines per 10 μm in all three conditions (control, 10nM or 1mM spadin). From these experiments, we measured the proportion of mature spines (mushroom and cup shaped) and immature spines (thin and filopodia) (Figure 4B) and observed that spadin significantly increased the proportion of mature spines at either 10 nM or 1 μM, compared with control conditions (Figure 4D). Concurrently, the amount of immature spines was significantly decreased by either concentration of spadin (Figure 4E).

Spadin incubation also decreased the immature spine length, compared with that under control, untreated, conditions (Figure 5A and B). We quantified the length of mature spines and observed that spadin had no effect on this parameter (Figure 5C and D). However, analysis of mushroom head sizes showed that spadin increased this parameter, compared with control conditions (Figure 5E and F). These data indicated that spadin promoted the maturation of dendritic spines.

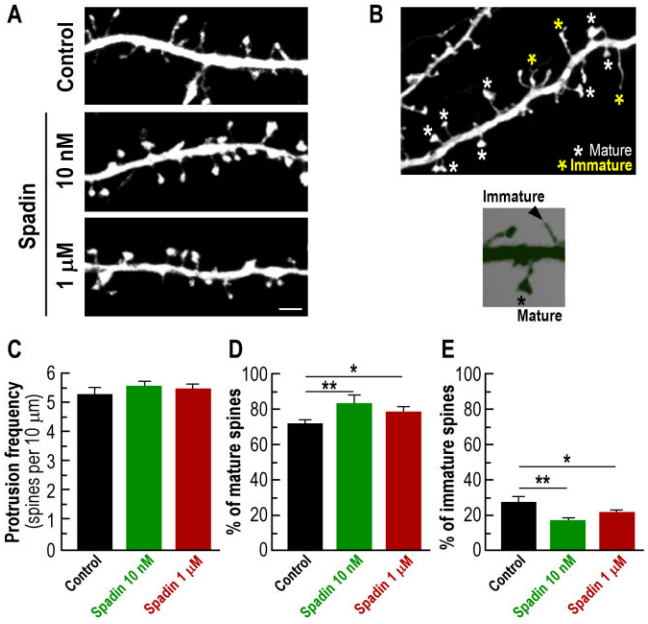

Figure 4

Spadin promotes spine maturation. (A) Representative images of dendrites from eGFP-transduced mouse cortical neurons either untreated (control) or treated with spadin 10 nM or 1 µM for 18 days. Scale bar, 2 µm. (B) Examples of mature and immature spines used in the analyses. (C) Histograms show quantification of protrusion frequency indicating that spadin does not affect spine density. (D and E) Bars show the percentage of mature or immature spines from dendrites of neurons revealing that spadin treatments significantly increase spine maturation. *P < 0.05, **P < 0.01, significantly different from control.

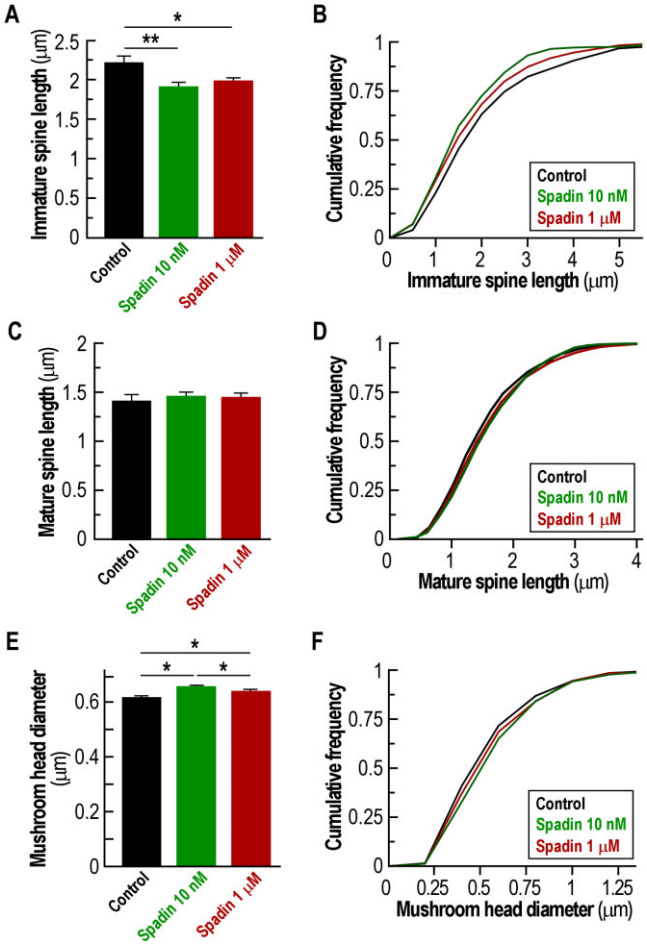

Figure 5

Spadin modifies spine length and mushroom head diameter. (A and B) Analysis of immature spine length. Graphs show quantification of immature spine length on neurons treated with 10 nM or 1 µM spadin. *P < 0.01, **P < 0.001, significantly different from control, K–S test. (C and D) Histograms show quantification of mature spine length and indicate that spadin did not affect spine density. Analysis of mature spine length. Graphs show quantification of mature spine length on neurons treated with 10 nM or 1 µM spadin. (E and F) Spine head diameter is increased in spadin-treated neurons. Graphs show quantification of mushroom type head diameter on neurons treated with 10 nM or 1 µM spadin for 18 days. *P < 0.05, significantly different from control, K–S test.

Spadin promotes synaptogenesis in vivo

We also examined the effect of spadin *in vivo* and specifically in cerebral areas involved in depression (i.e. prefrontal cortex and hippocampus) following i.v. administration of the peptide. We gave a daily i.v. injection of 100 µL of 1 µM spadin for 4 days, to assess the effect of spadin *in vivo* on synaptogenesis. Brain structures were dissected and analysed 7, 14 and 21 days after the first injection. Within the prefrontal cortex, spadin significantly increased the mRNA expression level of BDNF after 21 days, but not those of PSD-95 and synapsin (Figure 6A). By contrast, analysis of mRNA levels of PSD-95, synapsin and BDNF in the hippocampus revealed a significant increase in both synaptic markers (PSD-95 and synapsin; P < 0.05) and increased BDNF was more rapidly detected 7 and 14 days after the first spadin injection (P < 0.05; Figure 6B). We also observed that the protein levels of PSD-95 and synapsin were not modified within the prefrontal cortex (Figure 6C), but were significantly increased in the hippocampus 21 days after the first injection of spadin (Figure 6D). Interestingly, the BDNF protein content was enhanced from 7 to 21 days, but only in the hippocampus (Figure 6D). To compare results obtained from *in vitro* and *in vivo* studies, we performed qPCR experiments to determine the expression levels of synaptic proteins and BDNF from post-natal day 1 to adult mouse brain and observed that both PSD-95 and synapsin were expressed in all stages analysed, with a slight increase of their expression from days 1 to 15 (Supporting Information Fig. S3). By contrast, the level of BDNF was weak between days 1 and 6 and reached its peak expression at day 15. These results indicated that synaptic proteins and BDNF are expressed during embryonic and post-natal development, as well as in adult mice.

Altogether, our data confirmed that spadin was able to cross the blood–brain barrier and to trigger effects in the CNS, after injection in the periphery. These effects were correlated with a significant activation of synaptogenesis and an increase in BDNF content by spadin, particularly in the hippocampus.

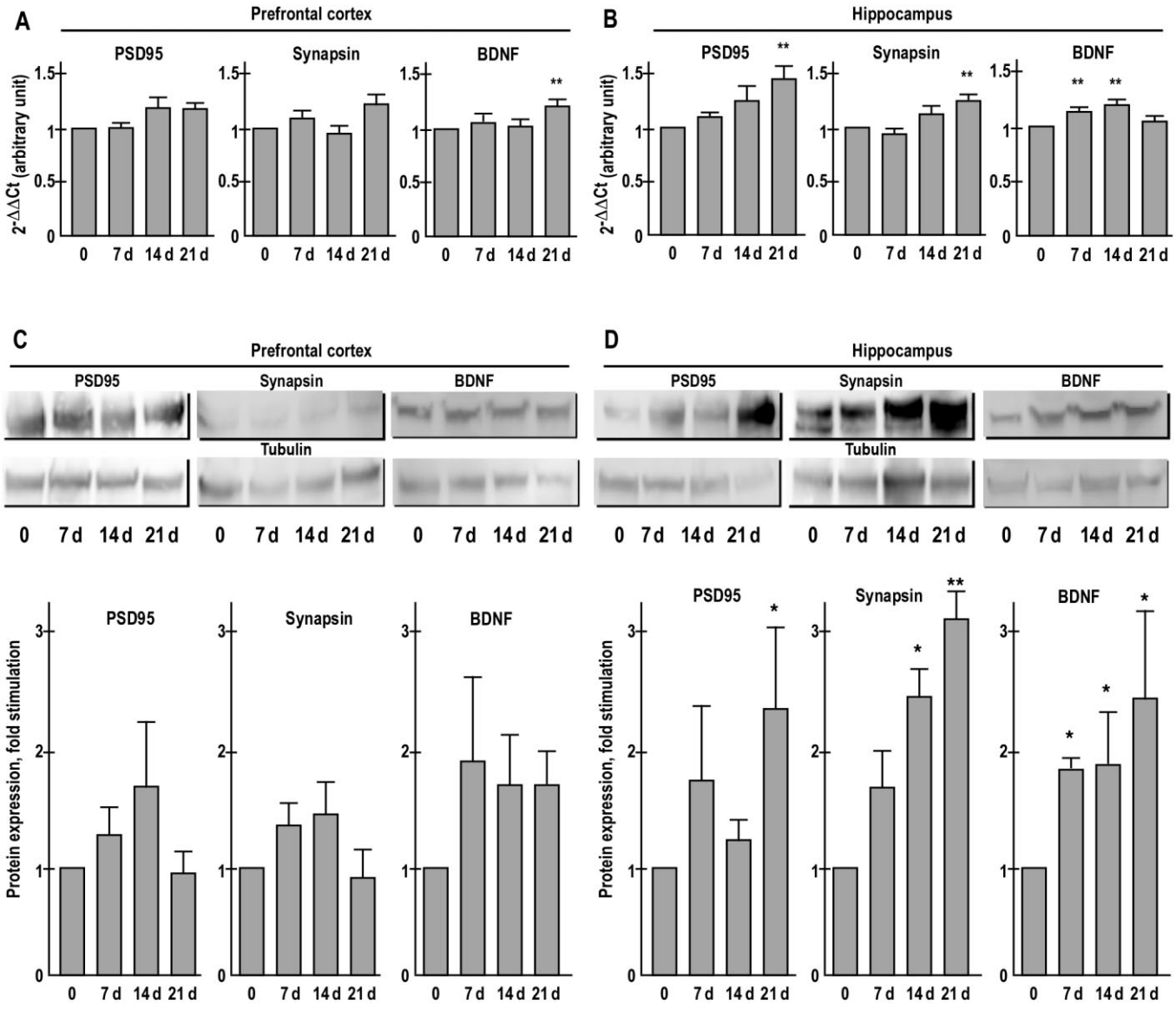

Figure 6

In vivo effects of spadin on synaptic proteins. Males C57BL/6J mice were injected in the caudal vein with 100 μL of 1 μM spadin once daily, for four days, then groups of mice were killed on days 7, 14 and 21 after the first injection. The brain was removed and prefrontal cortices and hippocampi were dissected and analysed by qPCR (A and B) and Western blotting (C and F). (A and B) RNA extracted from the prefrontal cortex (A) or the hippocampus (B) at the indicated day was subjected to quantitative PCR. Bar graphs showing the mRNA expression of PSD-95, synapsin and BDNF were normalized with the control condition (0) and compared with mice treated for 21 days with fluoxetine. Histograms are mean ± SEM from five independent determinations. *$P < 0.05$, significantly different from control (day 0). (C and D) Proteins extracted from the prefrontal cortex (C) or the hippocampus (D) recovered at the indicated day were subjected to Western blot analysis. Immunoblots shown are from a typical experiment. The amount of PSD-95, synapsin and BDNF expressed in the prefrontal cortex (C) and in the hippocampus (D) was represented as fold increase compared with control conditions. Data are means ± SEM from five independent experiments. *$P < 0.05$, **$P < 0.01$, significantly different from control (day 0).

Discussion and conclusions

Here we have investigated the *in vitro* and *in vivo* actions of spadin, a new type of antidepressant compound, at both molecular and cellular levels. Spadin binding to neurons caused neuronal depolarization and to the activation of MAP and PI3K signalling pathways. The latter pathway was involved in the protective effect of spadin against staurosporine-induced neuronal apoptosis. Furthermore, spadin treatment increased the expression of the synaptic markers PSD-95 and synapsin and led to dendritic spine maturation. Injection (i.v.) of spadin for 4 days increased PSD-95 and synapsin protein levels in the hippocampus sampled after 21 days whereas increased BDNF expression was apparent only after 7 days. Our results suggested two phases to spadin action. The first rapid antidepressant effect is

triggered by the increase of BDNF and associated with the release of 5-HT from the dorsal raphe and with hippocampal neurogenesis (Mazella *et al.*, 2010). The second phase is likely to correspond to the maturation of new neurons identified by the increase of synaptic markers as well as an increase in spinogenesis (the present study).

The efficacy of spadin as an antidepressant derives from its biological characteristics as well as its mode of action. Indeed, the peptide sequence of spadin is part of the endogenous peptide of 44 amino acids (PE) released from the precursor form of the NTSR3/sortilin receptor (Munck Petersen *et al.*, 1999). The antidepressant action of spadin is observed after an acute injection and its action on neurogenesis appears only after a 4 day treatment (Mazella *et al.*, 2010) whereas existing antidepressant drugs need 21 days to induce neurogenesis. The antidepressant properties of spadin are due to its ability to block the K^+ channel TREK-1 (Mazella *et al.*, 2010) without any detectable side effect related to this channel (Moha Ou Maati *et al.*, 2012). Although we had already identified the potent antidepressant action of spadin associated with hippocampal neurogenesis, its pharmacological, molecular and cellular modes of action remained unknown.

Functional interaction of spadin with neurons

The biochemical and electrophysiological properties of spadin were initially characterized using heterologous transfected cells (Mazella *et al.*, 2010; Moha ou Maati *et al.*, 2011). Here, we used a more physiologically relevant system to investigate the molecular and cellular mechanisms of action of spadin. In neurons, spadin clearly binds to two binding components with affinities of 0.05 and 100 nM respectively. Taking into account the concentration of PE detected in the brain (about 10 nM), spadin is likely to triggers cellular effects through its high-affinity binding site. We previously identified two targets of spadin, one of them is NTSR3/sortilin, the protein from which the peptide is released after maturation, and the second one is TREK-1 (Mazella *et al.*, 2010). The binding of spadin to TREK-1 blocks the related K^+ current and induces cell-membrane depolarization (Figure 1C). This process is compatible with the inhibition of TREK-1 channels (Fink *et al.*, 1996) (Hughes *et al.*, 2006). Moreover, we observed that spadin affects the plasma membrane distribution of TREK-1 and sortilin as it binds and induces their internalization (Supporting Information Fig. S1). One known function of NTSR3/sortilin is the sorting of proteins, this observation strongly suggests that sortilin not only targets TREK-1 channels to the plasma membrane (Mazella *et al.*, 2010), but also participates in their concomitant internalization. Spadin totally inactivates TREK-1 by blocking and internalizing the channel, a process crucial for the antidepressant effect in mice (Heurteaux *et al.*, 2006b).

Spadin protects neurons from apoptosis by a mechanism dependent on PI3K pathway

Spadin stimulates both ERK1/2 and PI3K signalling pathways in a time- and concentration-dependent manner (Figure 2). The level of phospho-Akt remains surprisingly high after 60 min. Usually, by that time, the level returns to the basal value. This finding could explain the prolonged effects of spadin *in vivo* on synaptic proteins and for the mTOR-independent Akt stimulation induced by the peptide. The ERK1/2 and PI3K pathways are known to be involved in cell growth and cell survival respectively. The expression of TREK-1 is known to be protective against ischaemia (Heurteaux *et al.*, 2004) (Buckler and Honore, 2005) and potent TREK-1 openers protect brain from ischaemia in rodents (Duprat *et al.*, 2000) (Blondeau *et al.*, 2002) (Heurteaux *et al.*, 2006a). In this scheme, spadin, which blocks TREK-1 activity, should decrease the protective action of the channel. We observed that spadin efficiently protected neurons from cell death by reversing staurosporine-induced caspase-3 activation (Figure 2H). This effect was mediated through a PI3K signalling pathway, but not via the MAPK pathway as only the PI3K inhibitor LY294002 reversed the protective action of spadin (Figure 2H). The involvement of the PI3K pathway in neuronal protection has already been reported in several studies including neuroprotection induced by nicotine against colchicine-induced apoptosis (Huang *et al.*, 2012) and the protective action of extracellular progranulin against toxic insults (Xu *et al.*, 2011).

Our finding that spadin acted as a protective agent on cortical neurons suggests that this regulatory system is not so simple. The membrane components responsible for the spadin-induced anti-apoptotic effects remain to be identified. One candidate is NTSR3/sortilin and further experiments performed on neurons prepared from sortilin-KO mice are required to verify this hypothesis.

In vitro *and* in vivo *effects of spadin on synaptogenesis*

Spadin has been described to initiate hippocampal neurogenesis, probably through the activation of CREB (Mazella *et al.*, 2010). This action, which was also observed with fluoxetine (Ohira *et al.*, 2013), does not indicate that new neurons generated by the treatment are functional. The modulation of neurogenesis in the aetiology of depression is still a matter of debate. Indeed, although it is well known that antidepressant drugs induce hippocampal and cortical neurogenesis, blocking neurogenesis does not alter the improving actions of antidepressant drugs on mood (Bessa *et al.*, 2009). Thus, the role of neurogenesis could be to buffer stress response and depressive behaviour (Snyder *et al.*, 2011). Our observation that spadin increases the ratio of mushroom spine types suggests a beneficial adjustment of synaptic function, which could lead a significant action of the peptide on neuron maturation and consequently on synaptic plasticity.

In vitro, we observed a rapid increase in the mRNA and protein expression levels of two synaptic markers; PSD-95 and synapsin, but not of BDNF upon incubation with spadin (Figure 3). The lack of spadin effect on BDNF protein expression is likely to be due to the low number of neuronal cells expressing the neurotrophic factor in our cultures. Acute exposure of neurons to spadin enhances the proportion of mature dendritic spines (mushrooms) without significant changes in the total number of spines (Figure 4). We analysed synaptic proteins up to 21 days because this time should be enough to show effects, taking into account that we showed that a 4 day treatment with spadin was enough to increase the phosphorylation of CREB in the hippocampus. Phospho-CREB is known to be crucial for full maturation of new

neurons (Fujioka *et al.*, 2004). When phospho-CREB is measured where immature new neurons are observed, the expression of phospho-CREB, correlated with maturation, is increased up to 14 days after proliferation. We therefore assumed that 21 days was enough time to observe variations. However, our observations were in agreement with the initial observation that overexpression of PSD-95 is involved in the maturation of spines (El-Husseini *et al.*, 2000). The regulation of spine morphology is generally correlated with changes in neuronal activity (Yuste and Bonhoeffer, 2001). Indeed, based on the structure–stability–function relationships, dendritic spines are classified in two categories, small and large (Kasai *et al.*, 2003). Small spines are usually unstable and non-functional whereas large spines (i.e. mushrooms) are much more stable and maintain strong synaptic connections. Moreover, increasing the proportion of large long-lasting spines in hippocampal neurons is likely to facilitate long-term memory (Lippman and Dunaevsky, 2005). Although dendritic spines are dynamic structures (Lippman and Dunaevsky, 2005), the change in morphology together with the up-regulation of synaptic markers strongly suggest that spadin is a potent up-regulator of neuronal functions.

We also analysed the effect of the peptide on the expression of the two synaptic proteins and BDNF in two cerebral regions involved in the regulation of mood disorders: the prefrontal cortex and the hippocampus (Figure 6). A 4 day treatment with spadin significantly increased the hippocampal expression of both PSD-95 and synapsin, 21 days after the first spadin injection, but not in the prefrontal cortex (Figure 6). These results confirmed the action of spadin on cultured neurons and indicated that the hippocampus is likely to be one of its main cerebral targets. Note that a 21 day administration of the 5-HT reuptake inhibitor fluoxetine was without any effect on synaptic protein mRNA expression levels (not shown). However, experiments carried out using intrahippocampal infusion of fluoxetine did increase PSD-95 expression and synaptogenesis (Mogha *et al.*, 2012). This discrepancy is probably due to the difference in the mode of administration. Interestingly, the same spadin treatment increased BDNF expression in the hippocampus more rapidly (after 7 days) than expression of PSD-95 and synapsin (after 21 days). This effect is compatible with our previous observation that a 4 day treatment with spadin induced a potent antidepressive action and a marked neurogenesis in the hippocampus (Mazella *et al.*, 2010). This result is also in agreement with the observation that a hippocampus-specific increase in BDNF activity is involved in the improvement of cognitive symptoms of depression and in the facilitation of hippocampal neurogenesis (Airan *et al.*, 2007).

To date, antidepressants that are able to reverse synaptic dysfunctions have a limited efficacy and a delayed response ranging from several weeks to months. The recent discovery that ketamine, a non-competitive NMDA receptor antagonist, rapidly enhanced synaptogenesis and reversed synaptic deficits (Duman and Aghajanian, 2012), as well as the discovery of the peptide spadin which bears key properties of a potent antidepressant, may open new fields for treatment of mood disorders. However, in contrast to ketamine, which activates the mTOR pathway through ERK and PI3K pathways (Licznerski and Duman, 2013), the spadin action appears independent of mTOR signalling. This is in agreement with the antidepressant effect of extracts of Radix polygalae (the dried root of *Polygala tenuifolia*) on the modulation of glutamatergic synapses, independently of mTOR activation (Shin *et al.*, 2014). Akt is usually placed downstream of mTORC2 and upstream of mTORC1 (Bhaskar and Hay, 2007). However, after deletion of mTORC2 activity, the phosphorylation of Akt was still observed suggesting that mTORC2 is not placed uptstream of Akt (Shiota *et al.*, 2006). In this case, Akt can phosphorylate other substrates than mTORC1, such as NF-κB or GSK3β that are involved in cell protection or cell cycle (Liu *et al.*, 2009). Further studies are necessary to identify the downstream pathways involved in spadin-induced neuronal activation.

The increase in the expression of synaptic proteins upon spadin treatment both *in vitro* and *in vivo* is a key property that could have considerable effects on therapy of depression. In addition to its ability to cross the blood–brain barrier and to stimulate neurogenesis, spadin appears to be a molecule able to potentiate dendritic spine maturation and synapse formation and, consequently, reinforces our concept that spadin is a novel potent antidepressant.

Acknowledgements

This work was supported by the Centre National de la Recherche Scientifique and the Agence Nationale de la Recherche (ANR, ANR-13-SAMA-0002-02 and ANR-11-EMMA-0050-01). SMa was supported by grants from the Fondation pour la Recherche Médicale (Equipe labellisée # DEQ20111223747) and the Agence Nationale de la Recherche (ANR-2011-JSV4-0031). We also thank the French government for the 'Investments for the Future' LABEX 'SIGNALIFE' # ANR-11-LABX-0028-01 to SMa and ICST # ANR-11 LABX 0015 to CH. JV was supported by a CIFRE fellowship.

Author contributions

C. D., A. K., J. V., H. M. M., M. R., S. M. and J. M. performed the experiments. M. B., S. Ma., C. H. and J. M. conceived and designed the experiments. M. B., S. Ma., C. H. and J. M. contributed reagents/materials/analysis tools. C. D. and J. M. wrote the paper.

Conflict of interest

Authors declare that there is no financial conflict of interest.

References

Airan RD, Meltzer LA, Roy M, Gong Y, Chen H, Deisseroth K (2007). High-speed imaging reveals neurophysiological links to behavior in an animal model of depression. Science 317: 819–823.

Alexander SPH, Benson HE, Faccenda E, Pawson AJ, Sharman JL, Catterall WA *et al.* (2013a). The Concise Guide to PHARMACOLOGY 2013/14: Ion Channels. Br J Pharmacol 170: 1607–1651.

Alexander SPH, Benson HE, Faccenda E, Pawson AJ, Sharman JL, Spedding M *et al.* (2013b). The Concise Guide to PHARMACOLOGY 2013/14: Enzymes. Br J Pharmacol 170: 1797–1867.

Berton O, Nestler EJ (2006). New approaches to antidepressant drug discovery: beyond monoamines. Nat Rev Neurosci 7: 137–151.

Bessa JM, Ferreira D, Melo I, Marques F, Cerqueira JJ, Palha JA *et al.* (2009). The mood-improving actions of antidepressants do not depend on neurogenesis but are associated with neuronal remodeling. Mol Psychiatry 14: 764–773, 739.

Bhaskar PT, Hay N (2007). The two TORCs and Akt. Dev Cell 12: 487–502.

Blondeau N, Lauritzen I, Widmann C, Lazdunski M, Heurteaux C (2002). A potent protective role of lysophospholipids against global cerebral ischemia and glutamate excitotoxicity in neuronal cultures. J Cereb Blood Flow Metab 22: 821–834.

Boschmans SA, Perkin MF, Terblanche SE (1987). Antidepressant drugs: imipramine, mianserin and trazodone. Comp Biochem Physiol C 86: 225–232.

Brewer GJ, Torricelli JR (2007). Isolation and culture of adult neurons and neurospheres. Nat Protoc 2: 1490–1498.

Buckler KJ, Honore E (2005). The lipid-activated two-pore domain K + channel TREK-1 is resistant to hypoxia: implication for ischaemic neuroprotection. J Physiol 562 (Pt 1): 213–222.

Carlezon WA Jr, Duman RS, Nestler EJ (2005). The many faces of CREB. Trends Neurosci 28: 436–445.

Coppola T, Beraud-Dufour S, Antoine A, Vincent JP, Mazella J (2008). Neurotensin protects pancreatic beta cells from apoptosis. Int J Biochem Cell Biol 40: 2296–2302.

Dingemans AM, van den Boogaart V, Vosse BA, van Suylen RJ, Griffioen AW, Thijssen VL (2010). Integrin expression profiling identifies integrin alpha5 and beta1 as prognostic factors in early stage non-small cell lung cancer. Mol Cancer 9: 152–160.

Dolder CR, Nelson MH, Iler CA (2012). The effects of mirtazapine on sleep in patients with major depressive disorder. Ann Clin Psychiatry 24: 215–224.

Drevets WC, Zarate CA Jr, Furey ML (2013). Antidepressant effects of the muscarinic cholinergic receptor antagonist scopolamine: a review. Biol Psychiatry 73: 1156–1163.

Duman RS, Aghajanian GK (2012). Synaptic dysfunction in depression: potential therapeutic targets. Science 338: 68–72.

Duprat F, Lesage F, Patel AJ, Fink M, Romey G, Lazdunski M (2000). The neuroprotective agent riluzole activates the two P domain K(+) channels TREK-1 and TRAAK. Mol Pharmacol 57: 906–912.

Dwyer JM, Duman RS (2013). Activation of mammalian target of rapamycin and synaptogenesis: role in the actions of rapid-acting antidepressants. Biol Psychiatry 73: 1189–1198.

El-Husseini AE, Schnell E, Chetkovich DM, Nicoll RA, Bredt DS (2000). PSD-95 involvement in maturation of excitatory synapses. Science 290: 1364–1368.

Fagiolini A, Comandini A, Catena Dell'Osso M, Kasper S (2012). Rediscovering trazodone for the treatment of major depressive disorder. CNS Drugs 26: 1033–1049.

Fava M, Kendler KS (2000). Major depressive disorder. Neuron 28: 335–341.

Fink M, Duprat F, Lesage F, Reyes R, Romey G, Heurteaux C *et al.* (1996). Cloning, functional expression and brain localization of a novel unconventional outward rectifier K+ channel. EMBO J 15: 6854–6862.

Fujioka T, Fujioka A, Duman RS (2004). Activation of cAMP signaling facilitates the morphological maturation of newborn neurons in adult hippocampus. J Neurosci 24: 319–328.

Hervieu GJ, Cluderay JE, Gray CW, Green PJ, Ranson JL, Randall AD *et al.* (2001). Distribution and expression of TREK-1, a two-pore-domain potassium channel, in the adult rat CNS. Neuroscience 103: 899–919.

Heurteaux C, Guy N, Laigle C, Blondeau N, Duprat F, Mazzuca M *et al.* (2004). TREK-1, a K+ channel involved in neuroprotection and general anesthesia. EMBO J 23: 2684–2695.

Heurteaux C, Laigle C, Blondeau N, Jarretou G, Lazdunski M (2006a). Alpha-linolenic acid and riluzole treatment confer cerebral protection and improve survival after focal brain ischemia. Neuroscience 137: 241–251.

Heurteaux C, Lucas G, Guy N, El Yacoubi M, Thummler S, Peng XD *et al.* (2006b). Deletion of the background potassium channel TREK-1 results in a depression-resistant phenotype. Nat Neurosci 9: 1134–1141.

Honore E (2007). The neuronal background K2P channels: focus on TREK1. Nat Rev Neurosci 8: 251–261.

Huang X, Cheng Z, Su Q, Zhu X, Wang Q, Chen R *et al.* (2012). Neuroprotection by nicotine against colchicine-induced apoptosis is mediated by PI3K–Akt pathways. Int J Neurosci 122: 324–332.

Hughes S, Magnay J, Foreman M, Publicover SJ, Dobson JP, El Haj AJ (2006). Expression of the mechanosensitive 2PK+ channel TREK-1 in human osteoblasts. J Cell Physiol 206: 738–748.

Kasai H, Matsuzaki M, Noguchi J, Yasumatsu N, Nakahara H (2003). Structure–stability–function relationships of dendritic spines. Trends Neurosci 26: 360–368.

Kilkenny C, Browne W, Cuthill IC, Emerson M, Altman DG (2010). Animal research: reporting *in vivo* experiments: the ARRIVE guidelines. Br J Pharmacol 160: 1577–1579.

Krishnan V, Nestler EJ (2008). The molecular neurobiology of depression. Nature 455: 894–902.

Li N, Lee B, Liu RJ, Banasr M, Dwyer JM, Iwata M *et al.* (2010). mTOR-dependent synapse formation underlies the rapid antidepressant effects of NMDA antagonists. Science 329: 959–964.

Li N, Liu RJ, Dwyer JM, Banasr M, Lee B, Son H *et al.* (2011). Glutamate *N*-methyl-D-aspartate receptor antagonists rapidly reverse behavioral and synaptic deficits caused by chronic stress exposure. Biol Psychiatry 69: 754–761.

Licznerski P, Duman RS (2013). Remodeling of axo-spinous synapses in the pathophysiology and treatment of depression. Neuroscience 251: 33–50.

Lin YC, Koleske AJ (2010). Mechanisms of synapse and dendrite maintenance and their disruption in psychiatric and neurodegenerative disorders. Annu Rev Neurosci 33: 349–378.

Lippman J, Dunaevsky A (2005). Dendritic spine morphogenesis and plasticity. J Neurobiol 64: 47–57.

Liu P, Cheng H, Roberts TM, Zhao JJ (2009). Targeting the phosphoinositide 3-kinase pathway in cancer. Nat Rev Drug Discov 8: 627–644.

Martin S, Bouschet T, Jenkins EL, Nishimune A, Henley JM (2008). Bidirectional regulation of kainate receptor surface expression in hippocampal neurons. J Biol Chem 283: 36435–36440.

Mazella J, Zsurger N, Navarro V, Chabry J, Kaghad M, Caput D *et al.* (1998). The 100-kDa neurotensin receptor is gp95/sortilin, a non-G-protein-coupled receptor. J Biol Chem 273: 26273–26276.

Mazella J, Petrault O, Lucas G, Deval E, Beraud-Dufour S, Gandin C *et al*. (2010). Spadin, a sortilin-derived peptide, targeting rodent TREK-1 channels: a new concept in the antidepressant drug design. PLoS Biol 8: e1000355.

McEwen BS, Olie JP (2005). Neurobiology of mood, anxiety, and emotions as revealed by studies of a unique antidepressant: tianeptine. Mol Psychiatry 10: 525–537.

McGrath J, Drummond G, McLachlan E, Kilkenny C, Wainwright C (2010). Guidelines for reporting experiments involving animals: the ARRIVE guidelines. Br J Pharmacol 160: 1573–1576.

McKinney RA (2010). Excitatory amino acid involvement in dendritic spine formation, maintenance and remodelling. J Physiol 588 (Pt 1): 107–116.

Mogha A, Guariglia SR, Debata PR, Wen GY, Banerjee P (2012). Serotonin 1A receptor-mediated signaling through ERK and PKCalpha is essential for normal synaptogenesis in neonatal mouse hippocampus. Transl Psychiatry 2: e66.

Moha ou Maati H, Peyronnet R, Devader C, Veyssiere J, Labbal F, Gandin C *et al*. (2011). A human TREK-1/HEK cell line: a highly efficient screening tool for drug development in neurological diseases. PLoS ONE 6: e25602.

Moha Ou Maati H, Veyssiere J, Labbal F, Coppola T, Gandin C, Widmann C *et al*. (2012). Spadin as a new antidepressant: absence of TREK-1-related side effects. Neuropharmacology 62: 278–288.

Munck Petersen C, Nielsen MS, Jacobsen C, Tauris J, Jacobsen L, Gliemann J *et al*. (1999). Propeptide cleavage conditions sortilin/neurotensin receptor-3 for ligand binding. EMBO J 18: 595–604.

Nestler EJ, Barrot M, DiLeone RJ, Eisch AJ, Gold SJ, Monteggia LM (2002). Neurobiology of depression. Neuron 34: 13–25.

Norrholm SD, Ouimet CC (2001). Altered dendritic spine density in animal models of depression and in response to antidepressant treatment. Synapse 42: 151–163.

Ohira K, Takeuchi R, Shoji H, Miyakawa T (2013). Fluoxetine-induced cortical adult neurogenesis. Neuropsychopharmacology 38: 909–920.

Pacher P, Kecskemeti V (2004). Trends in the development of new antidepressants. Is there a light at the end of the tunnel? Curr Med Chem 11: 925–943.

Pawson AJ, Sharman JL, Benson HE, Faccenda E, Alexander SP, Buneman OP *et al*.; NC-IUPHAR (2014). The IUPHAR/BPS Guide to PHARMACOLOGY: an expert-driven knowledge base of drug targets and their ligands. Nucl Acids Res 42 (Database Issue): D1098–D1106.

Petersen CM, Nielsen MS, Nykjaer A, Jacobsen L, Tommerup N, Rasmussen HH *et al*. (1997). Molecular identification of a novel candidate sorting receptor purified from human brain by receptor-associated protein affinity chromatography. J Biol Chem 272: 3599–3605.

Rodriguez A, Ehlenberger DB, Dickstein DL, Hof PR, Wearne SL (2008). Automated three-dimensional detection and shape classification of dendritic spines from fluorescence microscopy images. PLoS ONE 3: e1997.

Sanacora G, Smith MA, Pathak S, Su HL, Boeijinga PH, McCarthy DJ *et al*. (2014). Lanicemine: a low-trapping NMDA channel blocker produces sustained antidepressant efficacy with minimal psychotomimetic adverse effects. Mol Psychiatry 19: 978–985.

Sarret P, Krzywkowski P, Segal L, Nielsen MS, Petersen CM, Mazella J *et al*. (2003). Distribution of NTS3 receptor/sortilin mRNA and protein in the rat central nervous system. J Comp Neurol 461: 483–505.

Shansky RM, Hamo C, Hof PR, McEwen BS, Morrison JH (2009). Stress-induced dendritic remodeling in the prefrontal cortex is circuit specific. Cereb Cortex 19: 2479–2484.

Shin IJ, Son SU, Park H, Kim Y, Park SH, Swanberg K *et al*. (2014). Preclinical evidence of rapid-onset antidepressant-like effect in radix polygalae extract. PLoS ONE 9: e88617.

Shiota C, Woo JT, Lindner J, Shelton KD, Magnuson MA (2006). Multiallelic disruption of the rictor gene in mice reveals that mTOR complex 2 is essential for fetal growth and viability. Dev Cell 11: 583–589.

Sicouri S, Antzelevitch C (2008). Sudden cardiac death secondary to antidepressant and antipsychotic drugs. Expert Opin Drug Saf 7: 181–194.

Snyder JS, Soumier A, Brewer M, Pickel J, Cameron HA (2011). Adult hippocampal neurogenesis buffers stress responses and depressive behaviour. Nature 476: 458–461.

Srinivasan V, Zakaria R, Othman Z, Lauterbach EC, Acuna-Castroviejo D (2012). Agomelatine in depressive disorders: its novel mechanisms of action. J Neuropsychiatry Clin Neurosci 24: 290–308.

Thase ME, Denko T (2008). Pharmacotherapy of mood disorders. Annu Rev Clin Psychol 4: 53–91.

Xu J, Xilouri M, Bruban J, Shioi J, Shao Z, Papazoglou I *et al*. (2011). Extracellular progranulin protects cortical neurons from toxic insults by activating survival signaling. Neurobiol Aging 32: 2326, e2325–2316.

Yuste R, Bonhoeffer T (2001). Morphological changes in dendritic spines associated with long-term synaptic plasticity. Annu Rev Neurosci 24: 1071–1089.

Zarate CA Jr, Singh JB, Carlson PJ, Brutsche NE, Ameli R, Luckenbaugh DA *et al*. (2006). A randomized trial of an *N*-methyl-D-aspartate antagonist in treatment-resistant major depression. Arch Gen Psychiatry 63: 856–864.

Supporting information

Additional Supporting Information may be found in the online version of this article at the publisher's web-site:

http://dx.doi.org/10.1111/bph.13083

Figure S1 Immunoprecipitation of NTSR3/sortilin or TREK-1 with their corresponding antibodies from cortical neurons pretreated with Sulfo-NHS-biotin before incubation with spadin (1 μM) for the indicated times. Immunoprecipitated internalized proteins were revealed using HRP-streptavidin.

Figure S2 Degradation of spadin and analysis of blood–brain barrier transit. (A) Time course of disappearance of spadin after incubation with cortical neurons (open symbols) or mouse serum (closed symbols) for the indicated times. Incubations were terminated by acidification (HCl 1N) and the peptide contents were analysed by reverse-phase HPLC. Values represent the amount of intact spadin recovered after HPLC and expressed as the percentage of the initial amount of incubated peptide. Values are means ± SEM of three independent determinations obtained from three different neurons preparations or sera samples. (B) Fluorescent Atto488-spadin crosses the blood–brain barrier. HPLC profile

of Atto488- spadin recovered in the brain 30 min after i.v. injection. The brain was subjected to acidic extraction and the extracted peptide content was analysed by reverse-phase HPLC. The retention time for spadin-Atto488 is indicated by the arrow.

Figure S3 Expression of PSD-95, synapsin and BDNF during mouse brain development. The brain (from mice; ages as indicated) was removed and cortical cortices were dissected and analysed in qPCR experiments. Bar graphs showing the mRNA expression of PSD-95, synapsin and BDNF from 1 (D1), 3 (D3), 6 (D6) and 15-day-old (D15) mice were compared with the expression levels of adult (Adt) mice. Histograms are mean ± SEM from three independent determinations.